Overcoming the Data Gap of Floating Photovoltaic Plants: Synthetic Data Generation and Transfer Learning Techniques

Leticia O. Santos[1], Breno B. Freitas[1], Tarek AlSkaif[2] and Paulo C. M. Carvalho[1]

[1] Electrical Engineering Department, Federal University of Ceará, Fortaleza (Brazil)

[2] Information Technology Group, Wageningen University & Research, Wageningen (Netherlands)

Abstract

The scarcity of data in newly-built photovoltaic (PV) systems, particularly floating PV (FPV) plants, presents challenges for performance estimation and forecasting. This study implements a physics-based model for synthetic data generation and a deep learning (DL)-based transfer learning technique to mitigate the problem of limited data in a new FPV plant. First, a transient physical model is calibrated using limited data from an FPV plant (7, 15, and 30 days) to generate synthetic data used to train a Long Short-Term Memory (LSTM) model. Second, a LSTM model is pre-trained with data from a conventional PV plant and fine-tuned using limited data from the FPV plant. Both approaches are compared and the LSTM model fine-tuned outperforms the model trained with synthetic data. However, the physical model provides acceptable performance even with minimal real data, showing a maximum MAE difference of 0.58 °C. This scale of difference in error translates into less than 0.1 % error in PV efficiency, demonstrating that synthetic data can serve as a reliable alternative when data from PV plants are not available.

Keywords: Synthetic data, transfer learning, floating PV, knowledge transfer, fine-tuning.

1. Introduction

One fundamental challenge in managing newly-built photovoltaic (PV) systems is the scarcity of data for performance estimation and forecasting. This challenge is particularly true for floating PV (FPV) plants, given their early stage of implementation (Micheli, 2021). A practical pathway is to use knowledge from existing plants (Schreiber, J., & Sick, B., 2023). Knowledge transfer techniques offer viable alternatives to reduce dependency on costly, hard-to-obtain real data and support PV monitoring, fault detection, storage solutions, grid integration, and DC/AC load management. In practice, techniques to mitigate limited data availability typically involve two steps, selecting an appropriate model and choosing a knowledge transfer technique for model adaptation, enabling accurate estimations for new site with few observations.

Models for PV applications are based on physical and data-driven methods. A physical model is a mathematical formulation based on the physical principles governing PV conversion. Physical models often incorporate energy balance, cloud dynamics, sky images or remote sensing. As a result, they can be computationally intensive, and their performance is constrained by the accuracy of weather data (Liu et al, 2024), and by the dependency on the PV plant design parameters (Ma et al, 2024). However, they offer interpretability, require little to no prior historical data, and can be applied for long-horizon predictions.

Unlike physical models, data-driven methods avoid reliance on PV plant parameters by learning mappings from predictors. Currently, machine learning (ML) and deep learning (DL) models became popular for capturing nonlinearities, while incorporate diverse features. However, traditional ML models (e.g., support vector machine, random forests, gradient boosting) and generic DL (e.g., fully-connected neural networks and convolutional neural networks (CNNs)) are powerful, but do not explicitly model temporal dependence in their standard forms (Zhang et al, 2023). Consequently, time-series oriented DL models have emerged to better encode trend and periodicity patterns in time series, long short-term memory (LSTMs) networks for instance, is one of the most popular representatives (Zhao et al, 2025). However, data-driven methods in general perform best when large-scale, high-quality training samples are available.

10.18086/swc.2025.03.48 Available at http://proceedings.ises.org

In practice, newly-built plants often lack sufficient data to implement data-driven methods, and models trained on one domain degrade under domain shift. This challenge is pronounced for emerging installations such as FPV, that present distinct thermal characteristics behavior relative to conventional PV plants. In such cases, a knowledge transfer technique for model adaptation is necessary to avoid poor generalization or negative transfer. One option is to use physical models to generate synthetic historical data, the resulting theoretical series enable data-driven training. Transfer learning (TL) is other option to mitigate this problem by leveraging related source plants to improve predictions at a target plant with limited data (Liao et al, 2023). Although TL does not require identical source and target distributions, it does assume relatedness between domains (Tang et al, 2022). Common TL techniques are instance-based (reweight/select source samples), feature-based (learn transferable representations to reduce distribution gaps), and parameter/model-based (sharing parameters or using regularizers to constrain the target model toward the source) (Liao et al, 2024).

A prominent TL technique is fine-tuning, which first pre-trains a model on source domain data and then finetunes its parameters based on target domain data. Fine-tuning with DL models such as CNNs, LSTMs, hybrid, and layer-wise techniques, has shown gains across PV sites, reducing compute versus training from scratch, and improving generalization (Tang et al, 2024). Additional TL techniques include instance-based ensembles that reweight predictions from neighboring plants (Niu et al, 2022), although this is limited to nearby plants and by privacy protection concerns (Lin et al, 2022). Also, representation learning (e.g., autoencoders) (Ju, Li & Sun, 2020), and unsupervised domain adaptation (e.g., maximum mean discrepancy-based) can help, but requires temporal alignment and robust scaling (Zhang et al, 2023). Emerging foundation-models, pre-trained on large, diverse datasets from multiple domains, promise broader generalization, but remain early-stage in PV applications and must be validated carefully to avoid negative transfer (Zhao et al, 2025).

While knowledge transfer techniques have been explored for PV power forecasting, application to FPV and in thermal performance estimation remains underexplored. This research contributes to fill this gap, our main contributions can be summarized as follows: (I) this study explores knowledge transfer techniques for PV module temperature (T_m) estimation in newly-built FPV plants; (II) two approaches are implemented: physics-based synthetic data generation, and a DL-based architecture for TL; (III) three different scenarios of limited data are analyzed to quantify the minimum amount of data from the target plant required for calibration. Historical data from a conventional PV plant is used to knowledge transfer to a newly-built FPV plant (with different thermal characteristics), addressing data scarcity and domain shift jointly.

The rest of the paper is organized as follows. Section 2 introduces the data, details the proposed models and knowledge transfer techniques. The results are presented in Section 3. Finally, the conclusions are drawn in Section 4.

2. Methodology

To overcome data scarcity in a newly-built FPV system (target plant) and estimate its operating T_m, historical meteorological data and data from a conventional PV system (source plant) are utilized. The problem statement is described in Subsection 2.1, followed by the two implemented approaches: physics-based synthetic data generation (Subsection 2.2) and a DL-based architecture for TL (Subsection 2.3). The data and experimental settings are detailed in Subsection 2.4.

2.1 Problem Statement

Before operation, a target plant typically has only historical predictor variables *(X)*, without corresponding labels *(Y)*. This reflects practical scenarios, as historical weather data can be obtained before the PV site becomes operational for feasibility studies. In Brazil, utility-scale PV projects require at least one-year of on-site solar resource measurements prior to obtaining authorization for operation (ANEEL 2023). The target domain dataset can therefore be denoted by Eq. 1.

$$\mathcal{D}_T = \left\{X_T^{(u)}\right\}_{u=1}^{n_T^{(u)}} \cup \left\{\left(X_T^{(l)}, Y_T^{(l)}\right)\right\}_{l=1}^{n_T^{(l)}} \tag{Eq. 1}$$

Where the first set $\{X_T^{(u)}\}$ corresponds to historical features available before operation (unlabeled), and the second set $\{(X_T^{(l)}, Y_T^{(l)})\}$ represents a limited number of labeled observations collected after the PV plant becomes operational. The terms $n_T^{(u)}$and $n_T^{(l)}$ denote the number of unlabeled (u) and labeled (l) samples, respectively. Since the number of labeled samples is typically insufficient for effective model training, accurate estimations for new PV sites are challenging. If a sufficiently large labeled dataset is available from a related source plant, defined as the source domain (Eq. 2), this prior knowledge encodes temporal and environmental patterns transferable to the target plant (Schreiber & Sick, 2023).

$$\mathcal{D}_S = \left\{\left(X_S^{(l)}, Y_S^{(l)}\right)\right\}_{l=1}^{n_{S}(l)} \quad \text{(Eq. 2)}$$

Where $n_S^{(l)}$ denote the number of labeled samples in the source domain.

2.2 Physics-Based Synthetic Data Generation

The first approach consists of generating a synthetic $T_m$time series for the target plant using a physical model. Limited labeled data obtained after the FPV plant becomes operational are used to calibrate the physical model. Model parameters are adjusted using different calibration periods (7, 15, and 30 days) to ensure that the generated synthetic data accurately reflects the thermal behavior of the FPV plant. The calibration dataset ($\mathcal{D}_T^{\text{calib}}$) corresponds to the subset of labeled samples in the target domain (Eq.1), represented by Eq. 3.

$$\mathcal{D}_T^{\text{calib}} \subseteq \left\{\left(X_T^{(l)}, Y_T^{(l)}\right)\right\}_{l=1}^{n_T^{(l)}} \quad \text{(Eq. 3)}$$

The calibrated model is then used to simulate historical T$_m$, yielding synthetic target values Y_T' used to complement the target domain. The resulting augmented dataset is defined by Eq. 4.

$$\mathcal{D}_T^{aug} = \left\{X_T{}^{(u)}, Y_T'{}^{(u)}\right\}_{u\,=\,1}^{n_T^{(u)}} \cup \left\{\left(X_T^{(l)}, Y_T^{(l)}\right)\right\}_{l=1}^{n_T^{(l)}} \quad \text{(Eq. 4)}$$

The physical model adopted is based on the transient energy balance of the PV system from Santos et al. (2024a), with parameters adapted for the floating modules and operational conditions of the target plant. This model was chosen due to its superior performance in estimating T$_m$ under local conditions, compared with classical physical models (Santos et al., 2024a).

The first subset of the augmented dataset $\left\{X_T{}^{(u)}, Y_T'{}^{(u)}\right\}_{u\,=\,1}^{n_T^{(u)}}$, corresponding to the synthetic T$_m$ time series, is then used to train an LSTM model. The LSTM architecture consists of two stacked recurrent layers with n_{units} neurons each, interleaved with dropout layers for regularization, followed by a dense layer with one single output node for T$_m$ estimation. Sequential samples are built using a 30-step sliding window to capture short- and mid-term temporal dependencies. Model hyperparameters, including the number of LSTM units, dropout rate, and batch size, are optimized via grid search. The training procedure employs *EarlyStopping* (patience = 5 epochs) and *ReduceLROnPlateau* (factor = 0.5, patience = 3) to prevent overfitting. Data are split chronologically (80% for training, 20% for validation). This pipeline (physical model for Y_T'+ LSTM), effectively combines physics and DL for T$_m$ estimation with limited labeled data, this workflow is illustrated in Figure 1.

2.3 Deep Learning-Based Transfer Learning

The second approach implements a DL-based TL framework to leverage prior knowledge from an existing PV plant. First, an LSTM model with the same architecture described in Section 2.2 is pre-trained on the source domain, $\mathcal{D}_S$ (Eq. 2), to capture temporal dependencies and T$_m$ dynamics. The resulting weights of the pre-trained model, denoted θ_S, represent a general baseline of PV thermal behavior under local environmental conditions.

Subsequently, the pre-trained model is fine-tuned using different periods (7, 15, and 30 days) of limited labeled data from the target plant, $\mathcal{D}_T^{\text{calib}}$ (Eq. 3). During fine-tuning, the two initial LSTM layers are frozen to retain the temporal knowledge from the source plant, while the remaining layers are updated using a reduced learning rate of 1×10^{-4}. This partial freezing enables domain adaptation to the target plant's distinct thermal behavior while preserving generalizable representations learned from the source plant.

Fine-tuning is performed for up to 20 epochs using *EarlyStopping* and *ReduceLROnPlateau*, with an internal temporal split (80% training, 20% validation) within the calibration dataset. Sequential samples are also constructed using 30-step sliding windows, and the same hyperparameters optimized during the pre-training stage are reused during fine-tuning to ensure architectural consistency and to avoid overfitting on short calibration periods. The adapted model weights after fine-tuning are denoted θ_T^{*}. This pipeline enables knowledge transfer from an existing PV plant to improve estimations for newly-built FPV plants, even with limited labeled data, this workflow is illustrated in Figure 1.

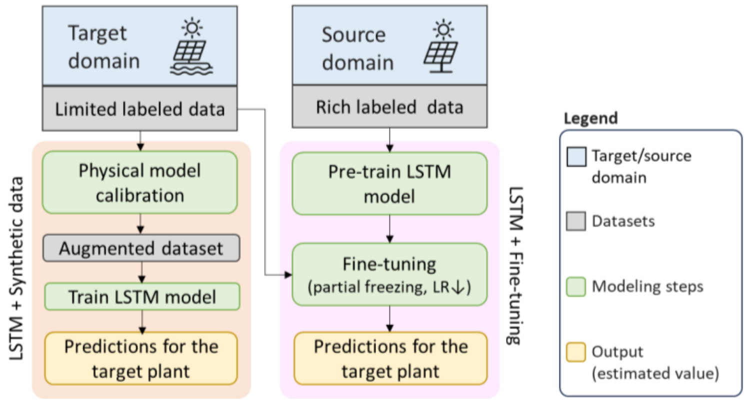

Figure 1: Techniques for T_m estimation in newly-built FPV plants: physics-based synthetic data generation, and transfer learning via fine-tuning.

2.4 Data and Experimental Settings

Meteorological and PV temperature data from both the source and target plants are used. The meteorological data come from a meteorological station at the Laboratory of Alternative Energies of the Federal University of Ceará (LEA – UFC). The meteorological variables used as predictor variables include solar irradiance, ambient temperature, and wind speed. Additionally, to consider temporal and sky information, the set of predictor variables is expanded with solar zenith and azimuth angles and the clear sky index. The conventional PV plant used as source plant is installed on the same campus as the newly-built FPV system, i.e., representative of the PV thermal behavior under the local meteorological conditions.

PV temperature data were collected directly on the PV modules with a dedicated monitoring system. The experimental campaign from the conventional PV plant is described in Assis et al. (2025), and was subsequently expanded to also monitor T_m of the new FPV plant. The raw data undergo a thorough quality control routine, data inspection identified no significant anomalies or outliers, predictor variables are normalized to [0, 1], using min-max scaling fitted on the training set values. One year of data (December 2022 - November 2023) is used to train the models. Three scenarios of limited data are simulated, considering 7, 15, or 30 days of data in December 2023 to calibrate the physical models when using the approach described in Sec. 2.2, or for fine-tuning when using the approach described in Sec. 2.3 A one-month period of data from the target plant, January 2024, is reserved exclusively for testing the models. All model development and training are performed in Python using the TensorFlow/Keras framework with the Adam optimizer. Models are trained with temporal ordering preserved to prevent data leakage. Performance is assessed on the test set using the Mean Absolute Error (MAE), Root Mean Square Error (RMSE), and coefficient of determination (R^2).

3. Results and Discussion

This section presents the results from the physics-based synthetic data generation and the DL-based architecture for TL in T_m estimation. Both approaches are evaluated in terms of predictive accuracy (MAE, RMSE, and R^2), temporal consistency, and robustness under limited calibration data, considering different training periods to determine the minimum amount of real data required for effective knowledge transfer. The metrics are shown in Table 1.

Table 1: Performance metrics for the LSTM models using synthetic data and transfer learning under different calibration periods.

	LSTM with Synthetic Data			LSTM with Transfer Learning		
	MAE	RMSE	R^2	MAE	RMSE	R^2
7 days	1.66	2.44	0.95	1.51	2.09	0.96
15 days	1.69	2.44	0.95	1.29	1.85	0.97
30 days	1.74	2.46	0.95	1.16	1.71	0.97

From the results presented in Table 1, the impact of the data period from the newly built FPV plant is beneficial when using LSTM with fine-tuning, where a gain of 0.35 °C in MAE is achieved when using 30 days of data compared to using 7 days. For the LSTM models trained with synthetic data from the physical model, no performance gain is observed. On the contrary, an increase of 0.08 °C in MAE is observed when 30 days are used to calibrate the physical model compared to the model calibrated with 7 days of data. These results further demonstrate that there is no need for long-term data to calibrate physical models, as they rely on physical correlations. A minimal amount of data, in this case, 7 days, is already sufficient to calibrate the parameters for a specific PV plant. Figure 2 presents the models' performance during the first test day.

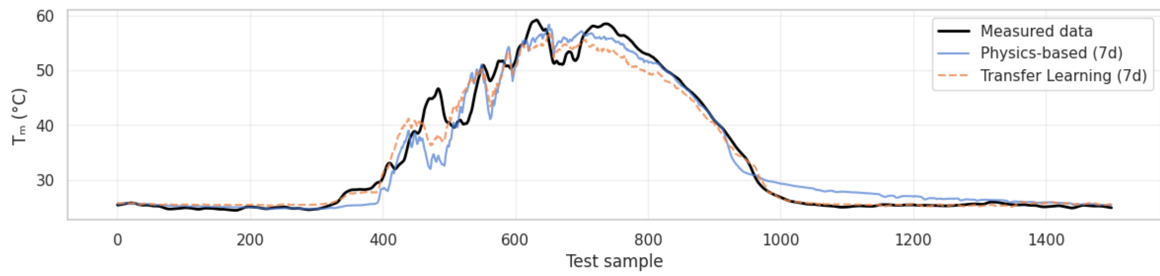

(a)

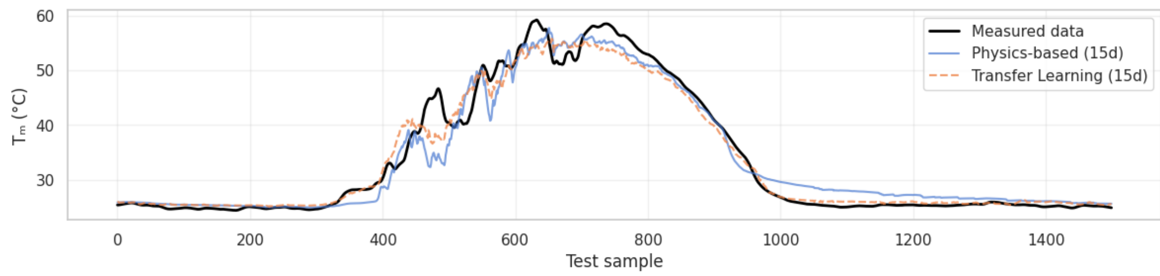

(b)

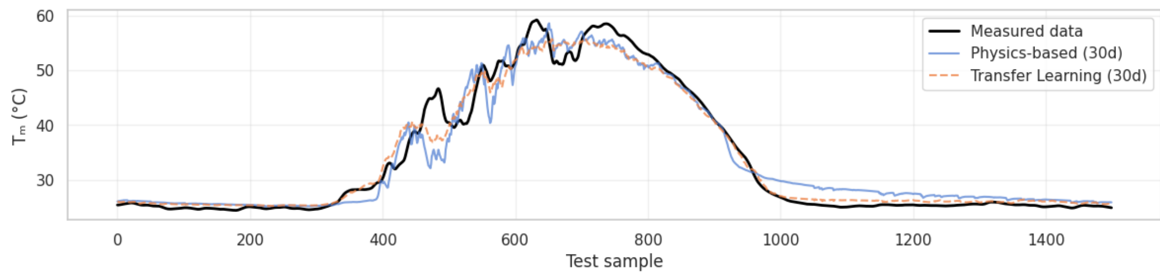

(c)

Figure 2: T_m estimation using a physics-based model for synthetic data generation and transfer learning via fine-tuning with 7 (a), 15 (b), and 30 (c) days of calibration.

Figure 2 shows the temporal correspondence on the first test day between the real T_m values and the model estimations for 7, 15, and 30 days. The models follow the temperature variations, and it can be observed that the curves of the DL-based TL models become closer to the real behavior as the amount of data used for fine-tuning increases. In contrast, physics-based models exhibit similar behavior regardless of the amount of calibration data. Additionally, the physics-based models show higher thermal inertia, which can be noticed by small delays at the beginning and end of the day, as well as by underestimations at temperature peaks.

To further understand the models' behavior, the residuals of the six models are compared. Figure 3 presents residual distributions (Predicted − Real) for each model. The physics-based models exhibit wider tails and slight asymmetries, indicating a slight underestimation of T_m. In contrast, the TL models show distributions more centered around zero and less dispersed. As the amount of calibration data increases (from 7 to 30 days), the distributions become narrower, indicating improved stability.

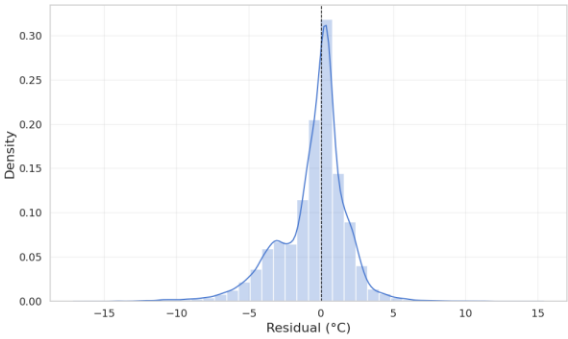

(a) Physics based (7 days)

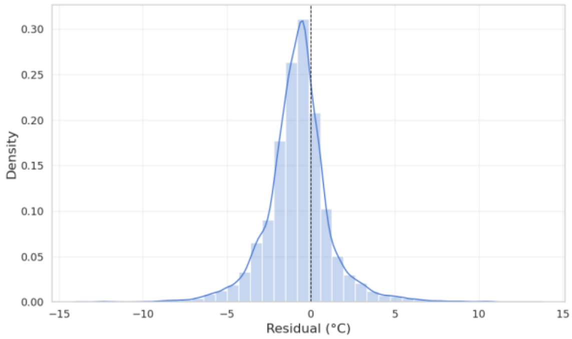

(b) DL-based TL (7 days)

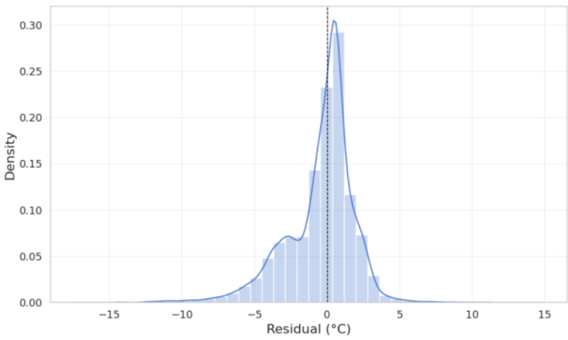

(c) Physics based (15 days)

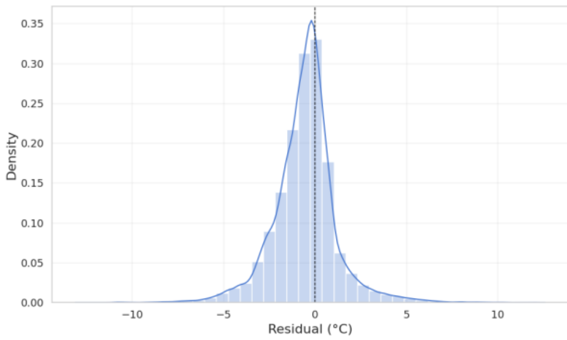

(d) DL-based TL (15 days)

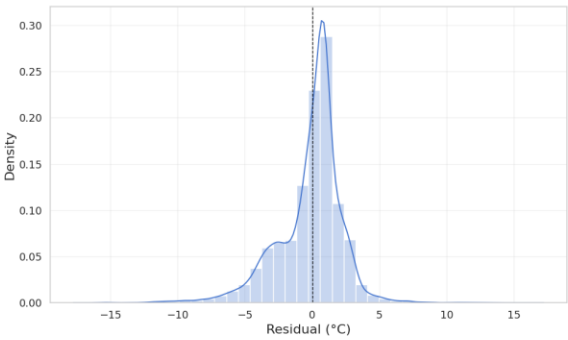

(e) Physics based (30 days)

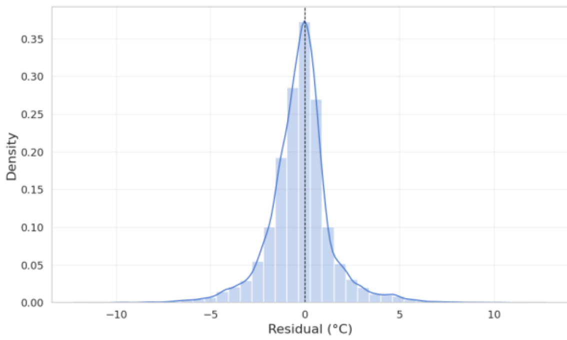

(f) DL-based TL (30 days)

Figure 3: Residual distributions (Predicted − Real) for the physics-based and DL-based transfer learning models under different calibration periods: (a–b) 7 days, (c–d) 15 days, and (e–f) 30 days.

Figure 4 shows the statistical alignment between the distributions of predicted and observed values. The 1:1 line represents the ideal reference (no bias). The physics-based model better follows the reference line in the 20–30 °C range. In the intermediate range (30–50 °C), the TL model is more consistent and smoother, following the reference line almost linearly. This indicates that the TL model has "learned" the typical patterns of medium temperature regimes. For temperatures above 50-55 °C, the physics-based model realigns more closely with the reference line, while the TL model tends to underestimate values in this range. In summary, the physics-based model is more reliable under thermal extremes, whereas the TL model performs better under intermediate and dynamic conditions. This complementary behavior suggests that a hybrid ensemble combining physics-based and data-driven estimations could further improve generalization across all operational ranges as sugested in Santos et al. (2024b).

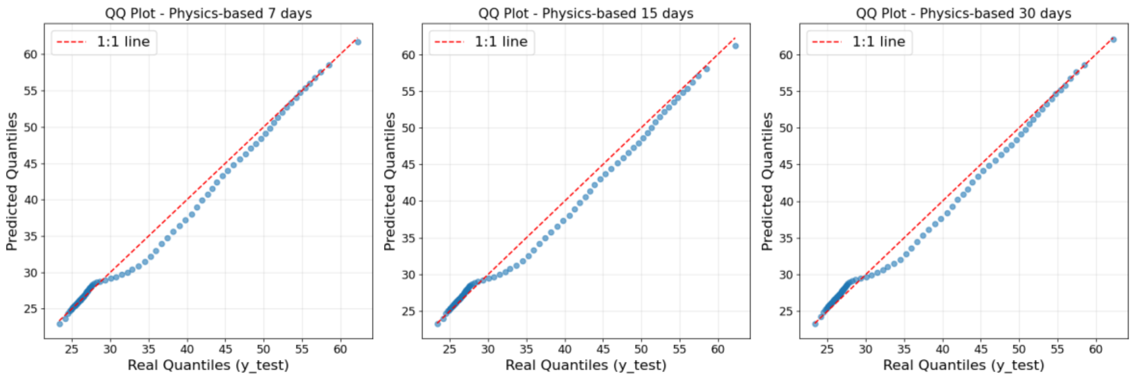

(a) (b) (c)

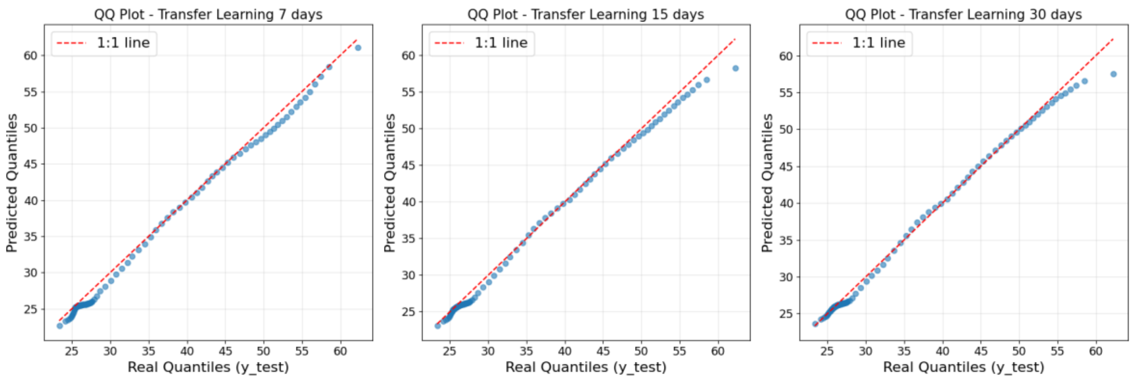

(d) (e) (f)

Figure 4: QQ plots comparing predicted and real T_m values for the physics-based and DL-based transfer learning models under different calibration periods: (a–c) physics-based models for 7, 15, and 30 days, and (d–f) DL-based TL models for 7, 15, and 30 days. The 1:1 line represents the ideal reference (no bias).

Overall, the LSTM models trained with data from a conventional PV plant and fine-tuned with limited data from the newly-built FPV plant show higher accuracy than the models trained solely with synthetic data. Even with only 7 days of data, the fine-tuned model already outperforms the physics-based model. However, the approach based on physical models for generating synthetic data presents a maximum MAE difference of 0.58 °C (for the 30-day case). Considering the temperature coefficient of −0.25 %/°C of the FPV modules, this difference translates into an error in PV efficiency of approximately 0.1 %. An advantage of the physics-based approach is that it does not necessarily require data from other PV plants (source plant), it only needs historical meteorological data and a limited amount of data from the newly-built plant for parameter optimization (an optional step, as the physical model can also be applied using generic parameters from the literature). In summary, both approaches provide acceptable performance for PV applications under limited data scenarios, with the LSTM fine-tuning approach performing better when data from another PV plant are available. However, depending on data availability, approach based on physical models to generate synthetic data may be advantageous since it does not rely on any prior PV plant data.

It is worth mentioning that the accuracy of both methods depends on their respective base models, as systematic errors can propagate from one domain to another. Therefore, the base model (either physical or source LSTM) must be carefully selected/developed. The methods presented here are extensible to other locations and installation types, such as building-integrated PV and agrivoltaic systems, as all these installations share physical similarities (PV conversion principles) but differ in terms of heat exchange with the surroundings.

4. Conclusion

This work addresses the data scarcity problem in a newly-built FPV plant by implementing and comparing two approaches for T_m estimation: physics-based synthetic data generation and DL-based TL via fine-tuning. Both approaches demonstrated satisfactory predictive performance (MAE < 2°C) using only limited labeled data, showing that accurate thermal modeling of new PV systems is feasible even under data-constrained scenarios.

The DL-based TL models, pre-trained on data from a conventional PV plant and fine-tuned with limited data from the new FPV plant, achieved higher accuracy and smoother temporal behavior than the physics-based synthetic data approach. However, the physics-based method presented competitive results with minimal calibration effort, highlighting its practical advantage when data from other plants are not available. The MAE difference between both approaches (0.58 °C at most) translates into less than 0.1 % error in PV efficiency, indicating that both strategies are viable for operational and planning applications in PV systems.

Future work can explore hybrid ensemble architectures that combine physics-based and data-driven estimations to leverage the complementary strengths of both methods, the capability of DL and fine tuning together with the physical consistency of synthetic models. Additionally, the framework can be tested also for PV power estimation and forecast, as well as on other PV installation types, such as building-integrated PV and agrivoltaic systems, to assess its adaptability across configurations with distinct heat exchange dynamics and environmental interactions.

5. Acknowledgments

The authors thank FUNCAP (*Fundação Cearense de Apoio ao Desenvolvimento Científico e Tecnológico*), linked to the Secretariat of Science, Technology and Higher Education of Ceará (SECITECE), for providing the doctoral grant to the first author, Coordenação de Aperfeiçoamento de Pessoal de Nível Superior (CAPES) - Finance Code 001 for the doctoral grant to the second author, and CNPq (*Conselho Nacional de Desenvolvimento Científico e Tecnológico*) for the research grant to the last author.

6. References

Agência Nacional de Energia Elétrica (ANEEL). *Resolução Normativa nº 1.071, de 29 de agosto de 2023* (Anexo II, item 8). *Diário Oficial da União*, 8 de setembro de 2023.

Assis, D. P., Santos, L. O., Carvalho, P. C. M., Pereira, R. I. S., Souza, J.J.S., 2025. Scalable Data Acquisition System for Real-Time Monitoring of Photovoltaic Plants, in IEEE Access, vol. 13, pp. 166787-166799. http://doi.org/10.1109/ACCESS.2025.3609654

Ju, Y., Li, J., Sun, G., 2020. Ultra-Short-Term Photovoltaic Power Prediction Based on Self-Attention Mechanism and Multi-Task Learning. IEEE Access, vol. 8, pp. 44821-44829. http://doi.org/10.1109/ACCESS.2020.2978635.

Liao, Q., Cao, D., Chen, Z., Blaabjerg, F., Weihao, H., 2023. Probabilistic wind power forecasting for newly-built wind farms based on multi-task Gaussian process method. Renew Energy, 217:119054. http://doi.org/10.1016/j.renene.2023.119054

Liao, R., Liu, Y., Xu, X., Li, Z., Chen, Y., Shen, X., Liu, J., 2024. Enhanced photovoltaic power generation forecasting for newly-built plants via Physics-Infused transfer learning with domain adversarial neural networks. Energy Conversion and Management, 322, 119114. http://doi.org/10.1016/j.enconman.2024.119114

Lin, J., Ma, J., Zhu, J., Liang, H., 2022. Deep domain adaptation for non-intrusive load monitoring based on a knowledge transfer learning network. IEEE Trans. Smart Grid, vol. 13, no. 1, pp. 280–292.

http://doi.org/10.1109/TSG.2021.3115910

Liu, J., Zang, H., Ding, T., Cheng, L., Wei, Z., Sun, G., 2024. Sky-image-derived deep decomposition for ultra-short-term photovoltaic power forecasting. IEEE Trans. Sustain. Energy, vol. 15, no. 2, pp. 871–883. http://doi.org/10.1109/TSTE.2023.3312401

Ma, T., Li, F., Gao, R., Hu, S., Ma, W., 2024. Short-term photovoltaic power forecasting based on a new hybrid deep learning model incorporating transfer learning strategy. Global Energy Interconnection, 7(6), 825-835. http://doi.org/10.1016/j.gloei.2024.11.010

Micheli, L., 2021. Energy and economic assessment of floating photovoltaics in Spanish reservoirs: cost competitiveness and the role of temperature. Solar Energy, 227, 625-634. http://doi.org/10.1016/j.solener.2021.08.058

Niu, T., Li, J., Wei, W., Yue, H., 2022. A hybrid deep learning framework integrating feature selection and transfer learning for multi-step global horizontal irradiation forecasting. Applied Energy, vol. 326, 119964. http://doi.org/10.1016/j.apenergy.2022.119964

Santos, L. O., Souza, F. A., Carvalho Filho, C. O., Carvalho, P. C., AlSkaif, T., Pereira, R. I., 2024a. Hybrid modeling for photovoltaic module operating temperature estimation. IEEE Journal of Photovoltaics, vol. 14, no. 3, 488-496. http://doi.org/10.1109/JPHOTOV.2024.3372328

Santos, L. O., AlSkaif, T., Barroso, G. C., Carvalho, P. C., 2024b. Photovoltaic power estimation and forecast models integrating physics and machine learning: A review on hybrid techniques. Solar Energy, vol. 284, 113044. https://doi.org/10.1016/j.solener.2024.113044

Schreiber, J., Sick, B., 2023. Model selection, adaptation, and combination for transfer learning in wind and photovoltaic power forecasts. Energy and AI, 14, 100249. http://doi.org/10.1016/j.egyai.2023.100249

Tang, Y., Yang, K., Zhang, S., Zhang, Z., 2022. Photovoltaic power forecasting: A hybrid deep learning model incorporating transfer learning strategy. Renewable and Sustainable Energy Reviews, 162, 112473. http://doi.org/10.1016/j.rser.2022.112473

Tang, Y., Yang, K., Zhang, S., Zhang, Z., 2024. Photovoltaic power forecasting: A dual-attention gated recurrent unit framework incorporating weather clustering and transfer learning strategy. Engineering Applications of Artificial Intelligence, 130, 107691. http://doi.org/10.1016/j.engappai.2023.107691

Zhang, Z., Wang, J., Xia, Y., Wei, D., Niu, Y., 2023. Solar-mixer: An efficient end-to-end model for long-sequence photovoltaic power generation time series forecasting. IEEE Trans. Sustain. Energy, vol. 14, no. 4, pp. 1979–1991. http://doi.org/10.1109/TSTE.2023.3268100

Zhao, P., Hu, W., Cao, D., Huang, R., Wu, X., Huang, Q., Chen, Z, 2025. Causal Mechanism-Enabled Zero-Label Learning for Power Generation Forecasting of Newly-Built PV Sites. IEEE Transactions on Sustainable Energy, vol. 16, no. 1, pp. 392-406. http://doi.org/10.1109/TSTE.2024.3459415